Neuron, Vol. 24, 803–808, December, 1999, Copyright ©1999 by Cell Press

Visualization of Synaptic Activity in Hippocampal Slices with FM1-43 Enabled by Fluorescence Quenching

Neurotechnique

Jason L. Pyle, Ege T. Kavalali,‡
Sukwoo Choi, and Richard W. Tsien†
Department of Molecular and Cellular Physiology
Beckman Center
Stanford University School of Medicine
Stanford, California 94305

Summary

Fluorescence imaging of presynaptic uptake and release of styryl dyes such as FM1-43 has provided valuable insights into synaptic function. However, in studies of CNS neurons, the utility of these dyes has been severely limited by nonsynaptic background fluorescence. This has thwarted the use of FM dyes in systems more intact than dissociated neuronal cultures. Here, we describe an approach to selectively reduce undesired fluorescence through quenching of the surface-bound FM1-43 signal. The introduction of sulforhodamine, a fluorophore that is not taken up by synaptic vesicles, selectively reduced the nonsynaptic fluorescence in FM1-43-labeled hippocampal cultures. When applied to rat hippocampal slices, this procedure allowed us to observe activity-dependent staining and destaining of functional synapses. Extending the usefulness of styryl dyes to slice preparations may help make functional synaptic networks amenable to optical measurements.

Introduction

Visual identification of synapses in living neuronal tissue has provided valuable insights into the functional organization of the nervous system (McMahan and Kuffler, 1971; Lichtman et al., 1987). Furthermore, the activity-dependent uptake of fluorescent molecules permits monitoring of presynaptic vesicle dynamics. This method exploits the endocytotic phase of activity-dependent fast vesicular recycling, a unique property of synapses, to load synaptic vesicles with fluorescent probes (Lichtman et al., 1985; Betz and Bewick, 1992).

The most commonly used fluorescent probes for this purpose are members of a family of styryl dyes exemplified by FM1-43 (Betz et al., 1996). FM1-43 and its congeners have yielded valuable insights into endocytotic and exocytotic mechanisms and have also proven useful in the visualization of active synapses (Cochilla et al., 1999). Styryl dyes display prominent fluorescence upon insertion of their hydrophobic tail into a lipid bilayer. The activity-dependent uptake of the FM dye into synaptic vesicles allows resolution of individual synaptic puncta in preparations such as the neuromuscular junction and cultured neurons (Betz and Bewick, 1992; Ryan et al., 1993). Unfortunately, FM1-43 staining and destaining has not been successfully implemented in more intact preparations such as brain slices. The large area of membrane lipid available for FM1-43 uptake and the tortuous pathway for its escape make it impractical to eliminate the large residual contribution of surface membrane-bound FM1-43. Despite extensive washing, nonspecific fluorescence from surface FM1-43 staining remains significant and overwhelms the intravesicular fluorescence signal. Similar problems can crop up even in hippocampal cultures due to nonspecific staining of acellular matter or membrane debris arising from cellular damage. Background fluorescence may often be bright enough to prevent adequate resolution of FM1-43-labeled synaptic puncta.

In either slices or cultures, it was of considerable interest to find a way to reduce nonspecific FM1-43 background fluorescence while preserving the fluorescent signal specifically arising from vesicular turnover. To do this, we took advantage of differences in the accessibility of fluorescent molecules nonspecifically staining surface membranes and those trapped in synaptic vesicles within the interior of nerve terminals. We reasoned that only FM1-43 molecules remaining on superficial membranes could be closely approached by soluble agents, delivered by extracellular application after stimulus-induced staining. In the simplest case, the quenching agent would remain at the cell exterior and not be taken up by synaptic vesicles during subsequent synaptic activity. Close-range interactions with this agent would then increase nonradiative transfer of absorbed energy from the excited surface fluorophore and thereby reduce its fluorescence emission. Thus, the unwanted signal could be minimized through fluorescence quenching.

Results

Sulforhodamine (S-Rhd), an aqueous fluorophore, has been used extensively as a fluorescent conjugate to many molecules of biological interest and as an acceptor for fluorescent resonance energy transfer (FRET) (Stryer, 1978). The absorption and emission spectra of S-Rhd peak at 586 and 605 nm, respectively (solid traces, Figure 1A), both peaks falling within the broad emission spectrum of FM1-43 (dashed trace). These spectral properties allowed us to use S-Rhd absorption to minimize unwanted FM1-43 fluorescence. The filtering strategy used an emission filter with a narrow bandpass at 540 $\pm$ 20 nm, a range of wavelengths over which FM1-43 emits but S-Rhd does not (Figure 1A, shaded panel). Following the addition of micromolar concentrations of S-Rhd, we observed a dramatic attenuation of the fluorescence from superficial membrane-bound FM1-43. However, if synaptic vesicles were stained by stimulation in the presence of FM1-43 and subsequently treated with S-Rhd, the FM1-43 sequestered within synaptic vesicles was largely sheltered from quenching.

The choice of S-Rhd was motivated by two requirements, that the quenching agent not damage neuronal

† To whom correspondence should be addressed (e-mail: rwtsien@stanford.edu).
‡ Present address: Department of Neuroscience, University of Texas Southwestern Medical Center, Dallas, Texas 75235.

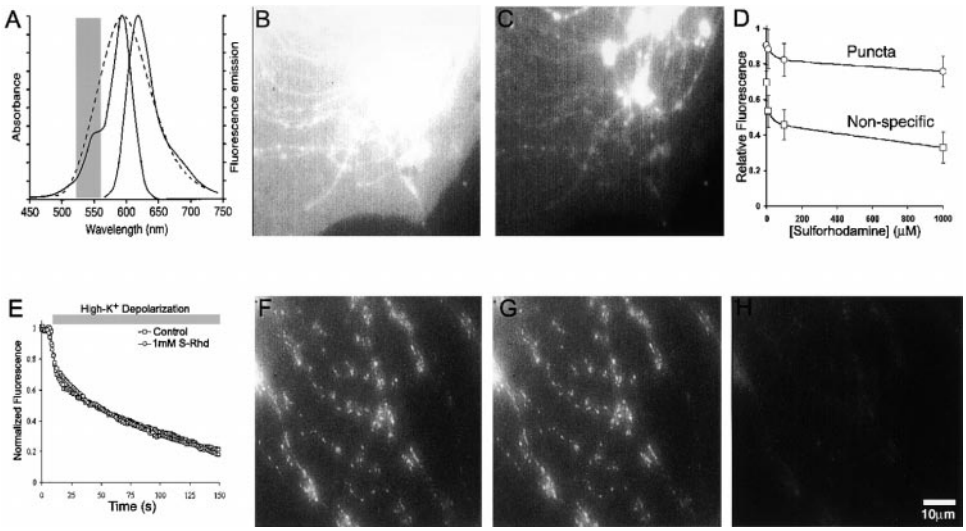

Figure 1. Sulforhodamine Preferentially Quenches Superficial FM1-43 Fluorescence in Hippocampal Cultures

(A) The broad emission spectrum of FM1-43 (dashed trace) superimposed on the excitation and emission spectra of S-Rhd (solid traces [Molecular Probes]). The gray bar indicates the bandwidth of our emission filter (540 ± 20 nm), a region where FM1-43 emission and S-Rhd excitation overlap. Here, we observed FM1-43 fluorescence free of S-Rhd emission.

(B) Intense fluorescence from nonspecific FM1-43 staining prevents visualization of the underlying activity-dependent staining of synaptic vesicles. Membranous debris stains brightly with FM1-43 in a nonspecific manner that will not abate even after prolonged washout.

(C) Same as (B) after the addition of 50 μM S-Rhd. Quenching of superficial FM1-43 fluorescence reveals the underlying synaptic staining. Synaptic origin of the remaining fluorescence was verified by activity-dependent destaining.

(D) Average of ($F_{FM1-43,\ S-Rhd}/F_{FM1-43}$) in similar experiments to those shown in (B) and (C). By comparison to nonspecific FM1-43 fluorescence (open square), S-Rhd has little effect on FM1-43 within synaptic puncta (open circles). Mean ± SEM, n = 78.

(E) Time course of FM1-43 destaining in the presence and absence of 1 mM S-Rhd in the same set of synaptic boutons. The presence of S-Rhd has no significant effect upon the ability of FM1-43 fluorescence to report synaptic vesicle cycling.

(F) A region of hippocampal culture stained with FM1-43 during high-K^+ depolarization. In contrast to (B), this region has clearly defined puncta with little nonspecific FM1-43 fluorescence.

(G) Same as (F) after addition of 100 μM S-Rhd. The pattern and intensity of FM1-43 fluorescence were largely unchanged.

(H) Subsequent high-K^+ depolarization of (G) in the presence of 100 μM S-Rhd. Activity-dependent loss of all FM1-43 fluorescence indicates that fluorescence seen after S-Rhd quenching was sequestered within synaptic vesicles.

preparations and that it not enter synaptic vesicles. We explored the use of several agents, including FM4-64, Nile Red, potassium bromide, potassium iodide, and potassium pyruvate, all of which have been used as quenchers of other fluorescent molecules. Each of these compounds proved unsuitable in our hands. The halides were clearly deleterious to hippocampal cells, the pyruvate salt failed to quench, and the Nile Red penetrated the neurons too easily. FM4-64 has already been used to quench FM1-43 fluorescence (Rouze and Schwartz, 1998) but has the property of being taken up into synaptic vesicles, potentially complicating the analysis of dye staining and destaining. S-Rhd is a well-characterized compound that is taken up by snake motor nerve endings (Lichtman et al., 1985) but not mammalian presynaptic terminals (J. Lichtman, unpublished data). Its localization can be directly monitored with fluorescence microscopy. Indeed, we tested S-Rhd in hippocampal cultures and confirmed that extracellular dye was well-tolerated by neurons and not taken up by synaptic boutons in sufficient quantity to produce detectable staining, even at external concentrations as high as 10 mM.

Reduction of Background in FM1-43-Stained Hippocampal Cultures

Hippocampal cultures labeled with FM1-43 following K^+ depolarization often display nonspecific background staining that partially or completely obscures fluorescence arising from synapses (Figure 1B). The addition of S-Rhd markedly reduced the overall fluorescence of such regions, allowing the resolution of discrete fluorescent puncta (Figure 1C) that could be destained with further K^+ depolarization (data not shown). The concentration dependence of S-Rhd's effect on FM1-43 fluorescence was studied systematically (Figure 1D). The overall concentration dependence was not linear as would have been expected if the quencher were simply extinguishing the light reaching the FM1-43 (inner filtering). Instead, the concentration dependence was biphasic. The reduction of fluorescence reached a plateau at <50 μM S-Rhd, as if a component of fluorescence associated with superficially accessible FM1-43 dye molecules had been fully ablated. The size of this component was significantly greater at nonsynaptic regions than at synaptic puncta. This would be expected if most of the FM1-43 at nonsynaptic regions were readily accessible to S-Rhd, while the bulk of the FM dye in synaptic boutons was sequestered.

We used hippocampal cultures to determine whether the presence of S-Rhd might alter the properties of FM1-43 as a reporter of vesicular exocytosis and recycling. The time course of K^+-induced destaining of FM1-43-labeled synapses was not significantly different in the presence or absence of S-Rhd (Figure 1E). In regions

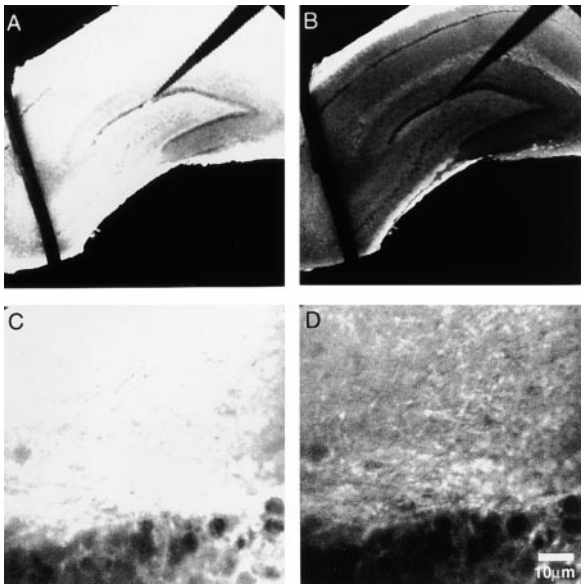

Figure 2. Sulforhodamine Quenches Superficial FM1-43 Fluorescence in Hippocampal Slices

(A) Confocal image of hippocampal slice stained with FM1-43 during high-K^+ depolarization.

(B) Same as (A) after addition of 50 μM S-Rhd. S-Rhd dramatically attenuated FM1-43 surface fluorescence.

(C and D) Higher magnification view of (A) and (B), respectively. These panels show the emergence of discrete fluorescent puncta near CA3 cell bodies following quenching with S-Rhd.

where FM1-43-labeled synaptic puncta could be studied with little interference from nonspecific fluorescence (Figure 1F), the application of 100 mM S-Rhd caused no appreciable change in the spatial organization or intensity of individual puncta (Figure 1G). However, by reducing the background staining, the S-Rhd had the salutory effect of improving the quality of the final images following destaining with high K^+ depolarization (Figure 1H).

Activity-Dependent Uptake and Release of FM1-43 in Hippocampal Slices

Previous attempts to demonstrate synaptic uptake and release of FM dyes in hippocampal slices have not been successful owing to nonspecific staining of the superficial surface of the slice. We set out to investigate whether the FM1-43 quenching observed with S-Rhd in cell culture would allow the visualization of synaptic puncta in slice preparations. Initially, fresh hippocampal slices were stained with high K^+ depolarization in the presence of FM143, followed by washout with dye-free solution. Even after prolonged washing (20–30 min), superficial nonspecific FM1-43 staining prevented the resolution of synaptic puncta (Figure 2A). A very different pattern of fluorescence emerged following application of S-Rhd (50 μM). The overall FM1-43 fluorescence across the slice surface was dramatically reduced (Figure 2B). A higher magnification view of the area near stratum lucidum is shown in Figures 2C and 2D. Here, the reduction of the previously saturated background fluorescence following S-Rhd application revealed well-defined fluorescent puncta (Figure 2D), similar in distribution to those previously visualized with immunofluorescence against synaptic markers (Dailey et al., 1994). In contrast, FM1-43-labeled puncta were not observed if the FM1-43 exposure was carried out in the absence of K^+ depolarization, thus indicating that the labeling was activity dependent.

In slices where puncta were identified with S-Rhd quenching, subsequent high K^+ depolarization produced a consistent decrease in the FM1-43 fluorescence of the puncta. This activity-dependent destaining is illustrated with images of area CA1 (Figure 3). FM1-43-stained puncta were seen with the help of S-Rhd quenching in dendritic fields neighboring the pyramidal cell layer (Figure 3A). Application of 90 mM K^+ solution caused a sharp drop in the fluorescence of the puncta (Figure 3B), as further documented with pooled data from 172 puncta (Figure 3F). On the other hand, the intensity of resolved puncta was not significantly reduced if continuous imaging and perfusion were carried out without exposure to high K^+ (data not shown), thus excluding side effects due to photobleaching and nonspecific dye loss. Surface debris that remained brightly stained in the presence of S-Rhd failed to lose fluorescence intensity during continuous perfusion, either with or without high K^+ (Figure 3F). In several cases, we attempted to restain slices with FM1-43 but found an unacceptably high level of background fluorescence, even with the benefit of S-Rhd quenching.

Further tests were performed to determine whether the FM1-43 destaining was linked to opening of voltage-gated Ca^{2+} channels, as would be expected for exocytotic turnover of synaptic vesicles. This work is illustrated with another experiment in CA1 (Figures 3C–3E). The fluorescent pattern found in dendritic regions at rest (Figure 3C) remained unchanged following application of high K^+ solution that contained Cd^{2+} (100 μM) to block all voltage-gated Ca^{2+} channels and thus decouple membrane depolarization from turnover of synaptic vesicles (Figure 3D). Upon washout of the Cd^{2+} to relieve Ca^{2+} channel blockade, further application of high K^+ solution caused a striking loss of fluorescence of the labeled synaptic terminals (Figure 3E).

Action Potential–Induced FM1-43 Turnover in Hippocampal Slices

While high K^+ depolarization provided a strong, global stimulus that was useful in establishing the feasibility of recording FM1-43 signals in hippocampal slices, we were particularly interested to see if the S-Rhd quenching approach would allow us to monitor synaptic activity evoked by action potentials. This would greatly expand the experimental usefulness of the technique. For this purpose, we focused on the mossy fiber input to hippocampal area CA3, a well-studied, spatially compact set of synaptic connections. Electrical activity of mossy fiber terminals in the proximal dendritic region of CA3 pyramidal neurons (stratum lucidum) was evoked by stimulation of mossy fiber axons with a bipolar stimulating electrode. To load recycling pools of presynaptic vesicles, the input tract was stimulated at 10 Hz for 120 s while the slice was bathed in FM1-43 (8 μM). Following

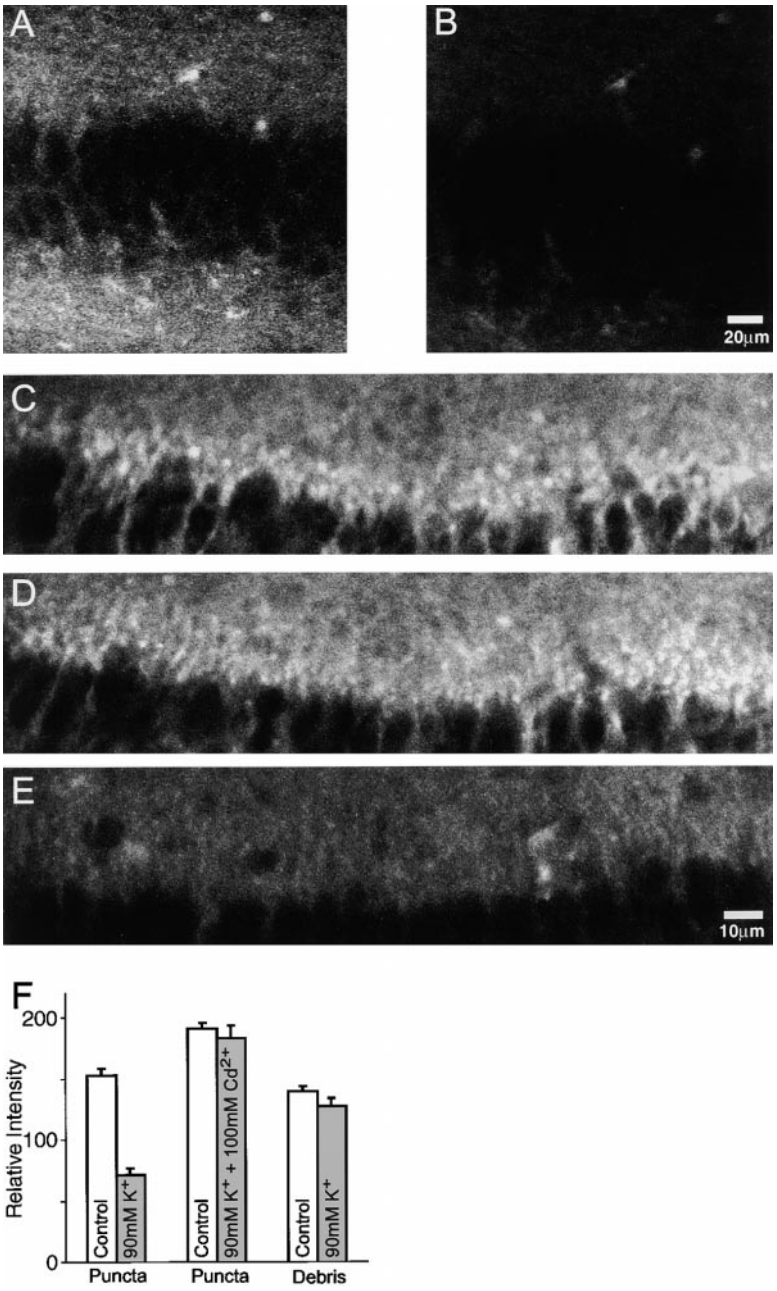

Figure 3. Fluorescent Staining in Hippocampal Slices Resolved with S-Rhd Quenching Is Activity Dependent

(A) High magnification view of CA1 region, showing regions neighboring pyramidal cell bodies of stratum pyramidale. Staining with FM1-43 during high-K^+ depolarization was followed by application of 50 μM S-Rhd as quenching agent.

(B) Same field as (A), after high-K^+ depolarization. A significant reduction in fluorescent intensity in both dendritic fields of CA1 pyramidal neurons occured during stimulation of presynaptic vesicle cycling.

(C) High magnification view of CA1 region after staining with FM1-43 and quenching with 50 μM S-Rhd. Discrete puncta were clearly resolved in the region of stratum radiatum.

(D) Same field as (C) after high-K^+ depolarization in the presence of 100 μM Cd^{2+}. With voltage-gated Ca^{2+} channels blocked, high-K^+ depolarization failed to reduce intensity of puncta.

(E) Same as (D) after washout of Cd^{2+} and subsequent high-K^+ depolarization. Recovery of voltage-gated Ca^{2+} channels permitted high-K^+ depolarization to destain fluorescent puncta.

(F) Pooled data from experiments where fluorescent puncta were stained and destained in hippocampal slices following S-Rhd quenching. Mean ± SEM. Open bars represent average levels of initial fluorescence before perfusion of depolarizing solution. Shaded bars show the residual fluorescence after application of depolarizing solution. Bars on the left show averaged data from 172 fluorescent puncta pooled from five separate experiments where hippocampal slices stained with FM1-43 were then destained by high-K^+ depolarization. In some experiments, a preceding high-K^+ challenge was performed in the presence of 100 μM Cd^{2+} ($n = 48$). Bars on the right represent identifiable debris that were stained with FM1-43 but failed to destain with high-K^+ depolarization in three separate experiments.

washout of FM dye and application of S-Rhd (50 μM), fluorescent puncta became visible within stratum lucidum, beneath the surface of the slice (Figure 4A). Further stimulation of the mossy fiber tract led to destaining of fluorescent puncta, as illustrated in Figures 4B–4D. Images taken after stimulation periods of 120 s (B), 360 s (C), and 720 s (D) showed a progressive loss of FM1-43 fluorescence. Destaining appeared to have reached a saturating level inasmuch as a subsequent bout of high-K^+ depolarization failed to cause any further loss of fluorescence (Figure 4E).

The kinetic profile of FM1-43 destaining, obtained with repeated imaging during action potential stimulation, is illustrated for 15 randomly selected fluorescent puncta (Figure 4F). The loss of fluorescence showed a broadly similar time course in all cases, with some degree of heterogeneity as previously reported for boutons in hippocampal cultures (Murthy et al., 1997). Pooled data from 67 puncta yielded a half-time for FM1-43 destaining of ~200 s.

Discussion

We have described a simple method that enables FM1-43 to be used in brain slices as a real-time marker of presynaptic vesicular turnover. The nonspecific background fluorescence that has precluded previous studies in situ was reduced by use of a quenching agent (S-Rhd) that readily penetrated into hippocampal slices where it sharply reduced the fluorescence of superficial

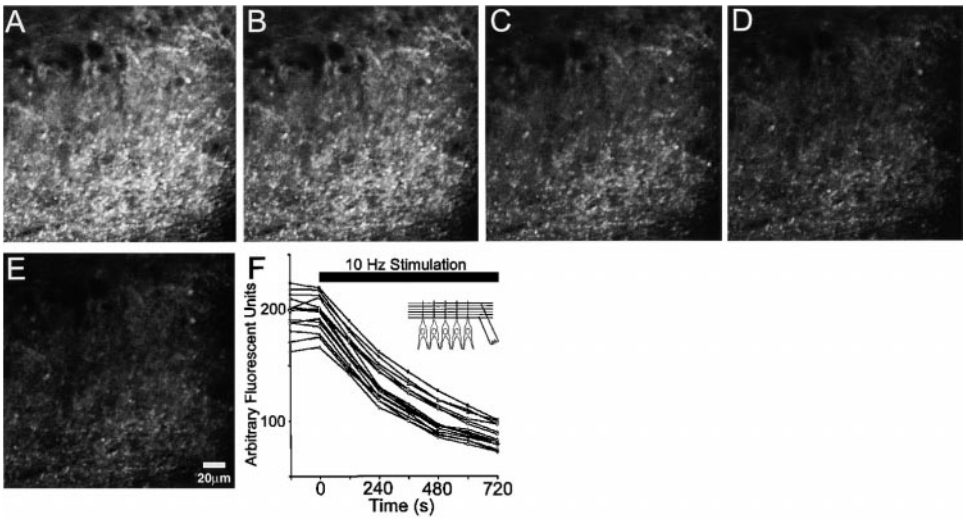

Figure 4. Time Course of Action Potential–Induced FM1-43 Destaining in Hippocampal Slices

(A) FM1-43-labeled synaptic puncta in stratum lucidum. The field of view is within the proximal dendrites of CA3 pyramidal cells (cell bodies appear as black ovals along the top). The mossy fiber tract was stimulated for 120 s at 10 Hz (300 mV, 200 μs pulse) with a bipolar electrode (shown schematically in [F], inset). Quenching with S-Rhd (50 μM) revealed FM1-43 staining of mossy fiber boutons.

(B–D) Same as (A) after 120, 360, and 720 s of bipolar electrode stimulation (10 Hz) in FM1-43 free solution. Stimulation of the mossy fiber tract results in intensity loss from fluorescent puncta in stratum lucidum as expected for action potential–driven exocytosis.

(E) After 720 s of bipolar electrode stimulation, a 120 s high-K^+ depolarization failed to further destain the preparation.

(F) Destaining time course of fifteen randomly selected fluorescent puncta in hippocampal slice. The inset, for schematic purposes only, depicts the bipolar stimulating electrode straddling the mossy fiber tract in stratum lucidum.

FM1-43 but not of dye molecules trapped within presynaptic vesicles. The validity of this approach was first established in hippocampal cultures in which S-Rhd strongly attenuated nonspecific FM1-43 fluorescence but left synaptic puncta brightly stained. The quenching effect reached saturation at low [S-Rhd], as expected for its interaction with a finite pool of externally accessible styryl dye. S-Rhd did not alter FM1-43 destaining kinetics. In hippocampal slices, which fully exemplified the problem of high background fluorescence, activity-dependent turnover of fluorescent dye was seen in both areas CA1 and CA3. FM1-43 was taken up and released by punctate structures of size and location appropriate to synaptic terminals in those regions (Dailey et al., 1994). Dye destaining was evoked by depolarization but not by extensive perfusion with basal medium or with depolarizing solutions that kept Ca^{2+} channels blocked. Vesicular turnover in FM-stained puncta corresponding to mossy fiber terminals could also be evoked by electrical stimulation of incoming axons.

Our estimate for the $t_{1/2}$ of FM1-43 destaining at mossy fiber synapses in the acute slice (~200 s) was much longer than the ~30 s half-time obtained with 10 Hz stimulation in isolated synapses of CA1-CA3 hippocampal cultures (Ryan and Smith, 1995; Klingauf et al., 1998). It would be interesting to find out whether the disparity between the two systems arises from differences in synaptic vesicle pool size, release probability, prevalence of rapid endocytosis, or some other factor. One interpretation that can be discounted is that the kinetics of fluorescence decay in the slice are distorted by restricted diffusion of dye molecules along tortuous extracellular pathways. Indeed, FM dye need not leave the slice in order for its exit from synaptic vesicles to be properly registered. It suffices for exocytosed dye molecules to bind to the vast excess of neighboring surface membranes, where their fluorescence would be immediately quenched by the ever-present S-Rhd. This represents a general advantage of our approach: the fluorescence of extraneous reporter dye can be straightforwardly and rapidly minimized even if the reporter molecules themselves remain trapped in the brain tissue. Further improvements in methodology might be made by examining a wider range of endocytotic markers and quenching molecules, including nonfluorescent agents.

The quenching approach is a significant step toward the ultimate goal of high-resolution imaging of presynaptic function within complex tissues (cf. Denk and Svoboda, 1997). By capitalizing on the advantages of multiphoton microscopy, it may be possible to refine the approach to the point of resolving the synapses of a single living axonal fiber, coursing through its native dendritic field. In principle, activity-dependent changes in presynaptic architecture might be visualized simultaneously with concomitant alterations in dendritic structures (e.g., Dailey and Smith, 1996; Ziv and Smith, 1996; Wu and Cline, 1998; Maletic-Savatic et al., 1999).

Experimental Procedures

Cell Culture

Hippocampal CA3-dentate gyrus regions were dissected from 1- to 2-day-old Sprague-Dawley rats. Neurons were dissociated by trypsin treatment (10 mg/ml for 10 min at 37°C) followed by trituration with a siliconized Pasteur pipette and then plated onto 12 mm coverslips coated with Matrigel. Culture media consisted of minimal essential media, 5 g/l glucose, 0.1g/l transferrin, 0.25 g/l insulin, 0.3 g/l glutamine, 5%–10% heat inactivated FCS, 2% B-27 supplement, and 2–4 μM cytosine arabinoside. Cultures were maintained at 37°C in a humidified incubator gassed with 95% air, 5% CO_2.

Slice Preparation

Young adult rats (30- to 45-day-old) were sacrificed by decapitation, and the brains were cooled in ice-cold aCSF containing (in mM) 120 NaCl, 3.5 KCl, 1.3 $MgCl_2$, 2.5 $CaCl_2$, 1.25 NaH_2PO_4, 26 $NaHCO_3$, and 11 glucose, gassed with 95% O_2/5% CO_2. Transverse hippocampal slices (300 μm) were cut in ice-cold aCSF using an automated vibroslicer. Brain slices from neonatal rats (6- to 8-day-old) were prepared using ice-cold modified aCSF containing (in mM) 194 sucrose, 20 NaCl, 3.5 KCl, 1.3 $MgCl_2$, 1.25 NaH_2PO_4, 26 $NaHCO_3$, and 11 glucose, gassed with 95% O_2/5% CO_2. Slices were then transferred into the imaging chamber, submerged, and superfused continuously at 2–4 ml/min with aCSF at room temperature. All experiments were conducted in the presence of NBQX (10 μM) to prevent synaptic transmission and recurrent activity during stimulation. To induce a discharge of action potentials, 200 μsec pulses of 30–300 μA currents (mainly 300 μA) were applied at a frequency of 10 Hz with bipolar stimulating electrode positioned close to the imaging sites on dendritic fields of interest.

FM1-43 Staining and Destaining in Cultures

A modified Tyrode solution (in mM): 150 NaCl, 4 KCl, 2 $MgCl_2$, 2 CaCl2, 10 Glucose, and 10 HEPES [pH 7.4]) was used as the extracellular medium for all experiments unless noted otherwise. The Tyrode solution always contained 10 μM NBQX to prevent recurrent action potentials. Synaptic boutons were loaded with 8 μM FM1-43 (Molecular Probes) in the presence of 45 mM K^+ and 2 mM Ca^{2+} for 90 s at room temperature. Individual boutons were imaged following 15 min of perfusion with dye-free Tyrode's solution. Depolarization-dependent destaining was obtained by application of 90 mM K^+ Tyrode solution after 15 min of perfusion with dye-free Tyrode's solution to wash out superficial FM1-43.

Fluorescence Microscopy

All fluorescent images of hippocampal cultures were acquired by a cooled and intensified CCD camera (Stanford Photonics). We used a Nikon 40×, 1.3 N. A. oil immersion objective on a Nikon Diaphot TMD microscope and excited FM dyes with 480/40 nm light (505 DCLP, 535/50 BP) for 66 ms through a computer-controlled optical switch (DX-1000, Stanford Photonics). Images were digitized using board and software from Axon Instruments. Circular regions of interest (ROI ~1.5 to 2 μm in diameter) were defined around the brightness center of mass of fluorescence spots. Pixel intensities within an ROI were averaged for each set of two consecutive frames to give one data point. If a displacement of a bouton was observed in subsequent frames, the entire data set was discarded. The relative loss of fluorescence (ΔF) for a given bouton was calculated as the difference between the average of 10 data points of baseline before a stimulus and the average of the last 10 data points of the time-lapse sequence. Vertical bars denote standard errors of the mean (SEM).

Confocal Microscopy

All images of slice preparations were aquired with standard confocal microscopy techniques. Confocal microscopy was performed using 4× air and 40× water immersion Zeiss objectives under a Sarastro Phoibos 1000 laser scanning system projecting into an upright Zeiss Axioskop. FM dyes were excited at 488 nm by a bandpass filtered argon laser. Fluorescence returned through a 520 nm DRLP was detected by a photomultiplier after additional excitation filtering and emission filtering at 540 ± 20 nm (Chroma Technology). Optical sections in hippocampal slices were taken approximately 25 μm beneath the cut surface. Images were acquired and analyzed by a Silicon Graphics Personal Iris running the Image Space software package (Molecular Dynamics).

Acknowledgments

We thank Jürgen Klingauf and Erika S. Piedras-Renteria for early discussions and helpful suggestions throughout this work and Stephen J. Smith and Lubert Stryer for helpful comments and constructive criticism. This work was supported by grants from the National Institute of Neurological Disease and Stroke, the National Institutes of Mental Health, the Mathers Charitable Trust, the National Institutes of Health Medical Scientist Training Program (J. L. P.), and the Dean's Postdoctoral Fellowship Fund (S. C.).

Received September 10, 1999; revised October 4, 1999.

References

Betz, W.J., and Bewick, G.S. (1992). Optical analysis of synaptic vesicle recycling at the frog neuromuscular junction. Science *255*, 200–203.

Betz, W.J., Mao, F., and Smith, C.B. (1996). Imaging exocytosis and endocytosis. Curr. Opin. Neurobiol. *6*, 365–371.

Cochilla, A.J., Angleson, J.K., and Betz, W.J. (1999). Monitoring secretory membrane with FM1-43 fluorescence. Annu. Rev. Neurosci. *22*, 1–10.

Dailey, M.E., and Smith, S.J. (1996). The dynamics of dendritic structure in developing hippocampal slices. J. Neurosci. *16*, 2983–2994.

Dailey, M.E., Buchanan, J., Bergles, D.E., and Smith, S.J. (1994). Mossy fiber growth and synaptogenesis in rat hippocampal slices in vitro. J. Neurosci. *14*, 1060–1078.

Denk, W., and Svoboda, K. (1997). Photon upmanship: why multiphoton imaging is more than a gimmick. Neuron *18*, 351–357.

Klingauf, J., Kavalali, E.T., and Tsien, R.W. (1998). Kinetics and regulation of fast endocytosis at hippocampal synapses. Nature *394*, 581–585.

Lichtman, J.W., Wilkinson, R.S., and Rich, M.M. (1985). Multiple innervation of tonic endplates revealed by activity-dependent uptake of fluorescent probes. Nature *314*, 357–359.

Lichtman, J.W., Magrassi, L., and Purves, D. (1987). Visualization of neuromuscular junctions over periods of several months in living mice. J. Neurosci. *7*, 1215–1222.

Maletic-Savatic, M., Malinow, R., and Svoboda, K. (1999). Rapid dendritic morphogenesis in CA1 hippocampal dendrites induced by synaptic activity. Science *283*, 1923–1927.

McMahan, U.J., and Kuffler, S.W. (1971). Visual identification of synaptic boutons on living ganglion cells and of varicosities in postganglionic axons in the heart of the frog. Proc. R. Soc. Lond. B Biol. Sci. *177*, 485–508.

Murthy, V.N., Sejnowski, T.J., and Stevens, C.F. (1997). Heterogeneous release properties of visualized individual hippocampal synapses. Neuron *18*, 599–612.

Rouze, N.C., and Schwartz, E.A. (1998). Continuous and transient vesicle cycling at a ribbon synapse. J. Neurosci. *18*, 8614–8624.

Ryan, T.A., and Smith, S.J. (1995). Vesicle pool mobilization during action potential firing at hippocampal synapses. Neuron *14*, 983–989.

Ryan, T.A., Reuter, H., Wendland, B., Schweizer, F.E., Tsien, R.W., and Smith, S.J. (1993). The kinetics of synaptic vesicle recycling measured at single presynaptic boutons. Neuron *11*, 713–724.

Stryer, L. (1978). Fluorescence energy transfer as a spectroscopic ruler. Annu. Rev. Biochem. *47*, 819–846.

Wu, G.Y., and Cline, H.T. (1998). Stabilization of dendritic arbor structure in vivo by CaMKII. Science *279*, 222–226.

Ziv, N.E., and Smith, S.J. (1996). Evidence for a role of dendritic filopodia in synaptogenesis and spine formation. Neuron *17*, 91–102.